Available online at www.sciencedirect.com
SCIENCE DIRECT®
Bioorganic & Medicinal Chemistry 14 (2006) 447–455
Bioorganic & Medicinal Chemistry

Enantiomers of *cis*-constrained and flexible 2-substituted GABA analogues exert opposite effects at recombinant $GABA_C$ receptors

Deborah L. Crittenden,[a,b] Anna Park,[b] Jian Qiu,[c] Richard B. Silverman,[d] Rujee K. Duke,[e] Graham A. R. Johnston,[e] Meredith J. T. Jordan[a] and Mary Chebib[b,*]

[a]*School of Chemistry, The University of Sydney, Sydney, NSW 2006, Australia*
[b]*Faculty of Pharmacy, The University of Sydney, Sydney, NSW 2006, Australia*
[c]*Replidyne Inc., 1450 Infinite Drive, Louisville, CO 80027, USA*
[d]*Department of Chemistry and Department of Biochemistry, Molecular Biology and Cell Biology and Centre for Drug Discovery and Chemical Biology, Northwestern University, Evanston, IL 60208-3113, USA*
[e]*Adrien Albert Laboratory of Medicinal Chemistry, Department of Pharmacology, The University of Sydney, NSW 2006, Australia*

Received 21 June 2005; revised 10 August 2005; accepted 10 August 2005
Available online 23 September 2005

Abstract—The effects of the enantiomers of a number of flexible and *cis*-constrained GABA analogues were tested on $GABA_C$ receptors expressed in *Xenopus laevis* oocytes using two-electrode voltage-clamp electrophysiology. (1*S*,2*R*)-*cis*-2-Aminomethylcyclopropane-1-carboxylic acid ((+)-CAMP), a potent and full agonist at the ρ1 ($EC_{50} \approx 40$ μM, $I_{max} \approx 100\%$) and ρ 2 ($EC_{50} \approx 17$ μM, $I_{max} \approx 100\%$) receptor subtypes, was found to be a potent partial agonist at ρ3 ($EC_{50} \approx 28$ μM, $I_{max} \approx 70\%$). (1*R*,2*S*)-*cis*-2-Aminomethylcyclopropane-1-carboxylic acid ((−)-CAMP), a weak antagonist at human ρ1 ($IC_{50} \approx 890$ μM) and ρ2 ($IC_{50} \approx 400$ μM) receptor subtypes, was also found to be a moderately potent antagonist at rat ρ3 ($IC_{50} \approx 180$ μM). Similarly, (1*R*,4*S*)-4-aminocyclopent-2-ene-1-carboxylic acid ((+)-ACPECA) was a full agonist at ρ1 ($EC_{50} \approx 135$ μM, $I_{max} \approx 100\%$) and ρ2 ($EC_{50} \approx 60$ μM, $I_{max} \approx 100\%$), but only a partial agonist at ρ3 ($EC_{50} \approx 112$ μM, $I_{max} \approx 37$ %), while (1*S*,4*R*)-4-aminocyclopent-2-ene-1-carboxylic acid ((−)-ACPECA) was a weak antagonist at all three receptor subtypes ($IC_{50} >> 300$ μM). 4-Amino-(*S*)-2-methylbutanoic acid ((*S*)-2MeGABA) and 4-amino-(*R*)-2-methylbutanoic acid ((*R*)-2MeGABA) followed the same trend, with (*S*)-2MeGABA acting as a full agonist at the ρ1 ($EC_{50} \approx 65$ μM, $I_{max} \approx 100\%$), and ρ2 ($EC_{50} \approx 20$ μM, $I_{max} \approx 100\%$) receptor subtypes, and a partial agonist at ρ3 ($EC_{50} \approx 25$ μM, $I_{max} \approx 90\%$). (*R*)-2MeGABA, however, was a moderately potent antagonist at all three receptor subtypes ($IC_{50} \approx 16$ μM at ρ1, 125 μM at ρ2 and 35 μM at ρ3). On the basis of these expanded biological activity data and the solution-phase molecular structures obtained at the MP2/6-31+G* level of ab initio theory, a rationale is proposed for the genesis of this stereoselectivity effect.

1. Introduction

γ-Aminobutyric acid (GABA), the major inhibitory neurotransmitter in the mammalian nervous system, is the endogenous ligand for three classes of GABA receptors; $GABA_A$, $GABA_B$ and $GABA_C$. $GABA_A$ receptors are ligand-gated chloride ion channels, which produce fast synaptic inhibition when activated by GABA. These receptors are inhibited by the alkaloid, bicuculline and modulated by barbiturates, steroids and benzodiazepines. In contrast, $GABA_B$ receptors activate G-protein-coupled second messenger systems, leading to the opening of calcium and potassium ion channels. They are insensitive to bicuculline and $GABA_A$ modulators but are selectively activated by (*R*)-baclofen and antagonized by its phosphonic and sulfonic analogues, phaclofen and saclofen, respectively. $GABA_C$ receptors are also ligand-gated chloride ion channels, but they are insensitive to both $GABA_A$ and $GABA_B$ ligands and high affinity modulators. Instead, they are selectively activated by (+)-*cis*-2-aminomethylcyclopropane-1-carboxylic acid ((+)-CAMP)[1] and blocked by (1,2,5,6-tetrahydropyridin-4-yl)methyl phosphinic acid (TPMPA).[2,3]

Keywords: GABA, γ-aminobutyric acid; (+)-CAMP, (1*S*,2*R*)-*cis*-2-aminomethylcyclopropane-1-carboxylic acid; (−)-CAMP, (1*R*,2*S*)-*cis*-2-aminomethylcyclopropane-1-carboxylic acid; (+)-ACPECA, (1*R*, 4*S*)-4-aminocyclopent-2-ene-1-carboxylic acid; (−)-ACPECA, (1*S*,4*R*)-4-aminocyclopent-2-ene-1-carboxylic acid; (*S*)-2MeGABA, 4-amino-(*S*)-2-methylbutanoic acid; (*R*)-2MeGABA, 4-amino-(*R*)-2-methylbutanoic acid.
* Corresponding author. Tel.: +61 2 9351 8584; fax: +61 2 9351 439; e-mail: maryc@pharm.usyd.edu.au

0968-0896/$ - see front matter © 2005 Elsevier Ltd. All rights reserved.
doi:10.1016/j.bmc.2005.08.037

Wild-type $GABA_C$ receptors are considered to be homo-oligomeric,[4,5] comprised of five identical ρ subunits. To date, two human ρ subunits (ρ1, ρ2)[6,7] and three rat ρ subunits (ρ1, ρ2 and ρ3)[8–11] have been cloned. The rat ρ3 subunit exhibits 63% and 61% amino acid sequence homology with the rat ρ1 and ρ2 subunits, respectively, which, in turn, exhibit 74% sequence homology with each other. Rat ρ1 and ρ2 subunits show 99% and 88% sequence homology to the human ρ1 and ρ2 subunits, respectively.[12]

Recombinant $GABA_C$ receptors have similar physiological and pharmacological properties to those of $GABA_C$ receptors found on native cells, indicating that these receptors may be homo-oligomeric in vivo. The use of reverse transcriptase PCR, Northern blot analysis and in situ hybridization techniques has shown that ρ1 $GABA_C$ receptors are concentrated in the retina, while ρ2 $GABA_C$ receptors appear to be more evenly distributed throughout the nervous system. $GABA_C$ receptors comprised of ρ3 subunits show a different distribution pattern, with lower expression levels in the retina and stronger expression levels in the hippocampus.[12–14] This difference in subtype distribution and physiological role increases the importance of developing subtype-specific $GABA_C$ receptor ligands.

Previous structure–activity relationship studies on ρ1 and ρ2 $GABA_C$ receptors, expressed in *Xenopus* oocytes, have led to the identification of a variety of useful compounds including TPMPA,[2,3] (+)-CAMP, *trans*-4-amino-2-methylbut-2-enoic acid (2-MeTACA)[1] and (±)-*trans*-2-aminomethylcyclopropane-1-carboxylic acid ((±)-TAMP),[15] that are used as pharmacological tools to study $GABA_C$ receptors.

TPMPA was the first selective $GABA_C$ receptor antagonist to differentiate $GABA_C$ receptors from $GABA_A$ and $GABA_B$ receptors,[2,3] and (+)-CAMP was shown to be the most selective agonist at human ρ1 and ρ2 $GABA_C$ receptors.[1] 2-MeTACA and (±)-TAMP were shown to functionally distinguish between homomeric ρ1, ρ2 and ρ3 $GABA_C$ receptors expressed in *Xenopus* oocytes.[15] These studies have also shown that GABA analogues can tolerate substitutions at the 2 position without loss of function,[16] although substitutions at the 3 and 4 positions cause loss of biological activity.[1,15,16] Substitution at the 2 position introduces a stereocentre to the molecule, resulting in the existence of two chemically distinct optical isomers. Previous studies, which involved testing of the optical isomers of CAMP for biological activity at ρ1 and ρ2 $GABA_C$ receptors, revealed that (+)-CAMP is a full agonist with negligible effects on $GABA_A$ or $GABA_B$ receptors, while (−)-CAMP is a weak $GABA_C$ receptor antagonist.

In the current study, we aim to contribute to the structure–activity relationships of optically pure chiral GABA analogues by expanding the range of compounds tested at $GABA_C$ receptors to include the enantiomerically resolved 4-amino-2-methylbutanoic acid (2-MeGABA) and 4-aminocyclopent-2-ene-1-carboxylic acid (ACPECA), which have previously only been tested as racemic mixtures.[16] These compounds will be tested at all three $GABA_C$ receptor subtypes. Furthermore, quantum mechanical modelling techniques will be used to provide insight into the likely three-dimensional solution-phase conformations of these conformationally restricted GABA analogues, which will then be used to interpret the experimental results and expand the existing structure–activity relationships.

2. Experimental results

Expression of the human ρ1 and ρ2 and rat ρ3 cRNA in *Xenopus laevis* oocytes generated GABA gated ion channels with similar conductance properties as described previously.[5,8,17] The electrostatic potential was clamped at −60 mV and the amplitudes of the whole-cell currents varied upon channel opening. For the ρ1 receptor, the currents ranged between 200 and 2000 nA. The magnitude of the current was an order of magnitude smaller for the ρ2 receptor, at around 20 nA. Whole-cell currents recorded from the ρ3 receptor ranged in magnitude from 50 to 2000 nA. The maximal GABA response was attained upon application of 100 μM GABA for the ρ1 and ρ2 receptors, whereas the ρ3 receptor required application of 300 μM GABA (Fig. 1).

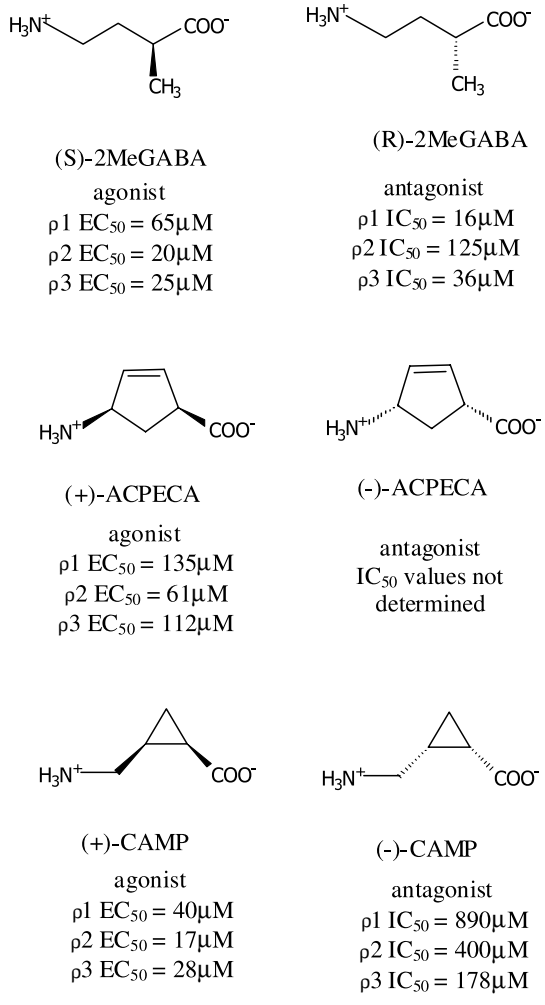

Figure 1. Structures of GABA analogues used in this study.

Agonist dose–response curves for all three receptor subtypes are shown in Figure 2. Antagonist dose–response curves are shown in Figure 3. The EC_{50} values, intrinsic activity (I_{max}), Hill coefficients (n_H) and IC_{50} values are summarized in Table 1.

(+)-CAMP, which has been shown previously to be a potent, full agonist at ρ1 and ρ2 receptors,[1] was a potent partial agonist at ρ3 (EC_{50} = 28.1 μM; I_{max} = 69.4 %). (−)-CAMP, in contrast, was a moderately potent antagonist at the ρ3 receptor (IC_{50} = 178 μM), which was two times more potent than at the ρ2 receptor (IC_{50} = 400 μM)[1] and five times more potent than at the ρ1 receptor (IC_{50} = 890 μM).[1]

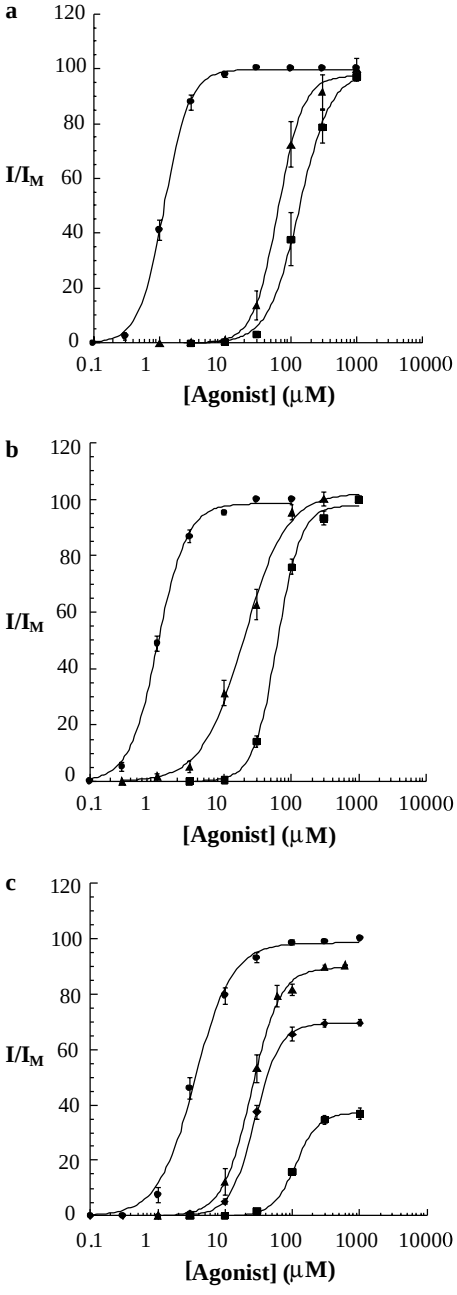

Figure 2. Dose–response curves for the agonists GABA (●), (+)-CAMP (♦), (*S*)-2MeGABA (▲) and (+)-ACPECA (■) at (a) ρ1, (b) ρ2 and (c) ρ3 $GABA_C$ receptors expressed in *Xenopus laevis* oocytes. Data are means ± SEM for n = 3–6 oocytes.

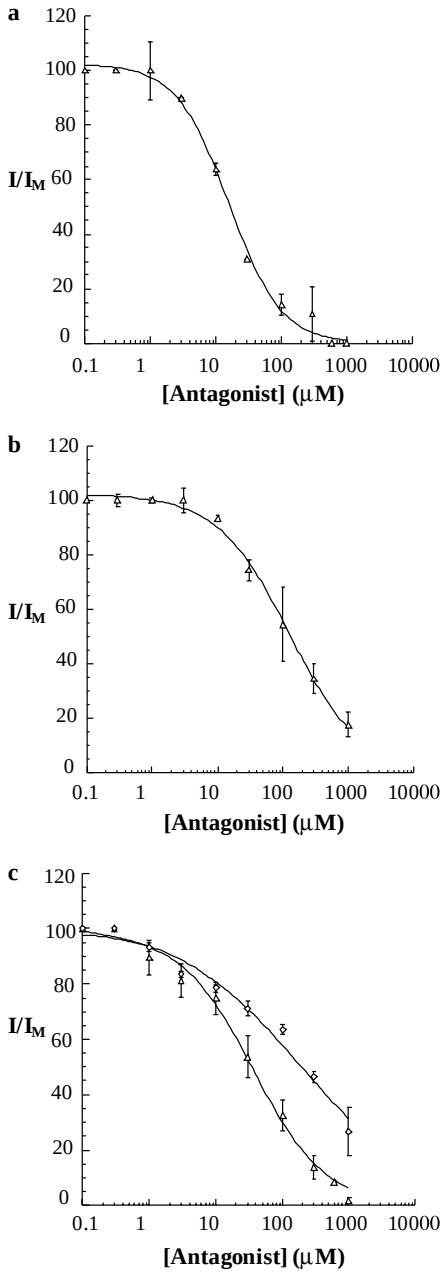

Figure 3. Inhibition curves for the antagonist (*R*)-2MeGABA (△) at (a) ρ1, (b) ρ2 and (c) ρ3 and (−)-CAMP (◊) at (c) ρ3 $GABA_C$ receptors expressed in *Xenopus Laevis* oocytes. Data are means ± SEM for n = 3–6 oocytes.

Like (+)-CAMP, (*R*)-2MeGABA was a potent, full agonist at ρ1 and ρ2 receptors (EC_{50} = 64.6 μM; I_{max} = 97.5% and EC_{50} = 19.8 μM; I_{max} = 102.1%, respectively) and a partial agonist at ρ3 (EC_{50} = 24.7 μM; I_{max} = 89.6%). (*S*)-2MeGABA was a potent antagonist at ρ1 and ρ3 (IC_{50} = 15.9 μM and IC_{50} = 35.8 μM, respectively) and a moderate antagonist at ρ2 (IC_{50} = 125 μM).

(+)-ACPECA was less potent than (+)-CAMP and (*R*)-2MeGABA, although similar trends in intrinsic activity were displayed among the subtypes. (+)-ACPECA was

Table 1. Effects of (+)-CAMP, (−)-CAMP, (*R*)-2MeGABA, (*S*)-2MeGABA, (+)-ACPECA and (−)-ACPECA at $GABA_C$ receptors expressed in *Xenopus* oocytes

Compound	Human ρ1 $GABA_C$ receptors			Human ρ2 $GABA_C$ receptors			Rat ρ3 $GABA_C$ receptors		
	EC_{50} (μM)	n_H	I_{max} (%)	EC_{50} (μM)	n_H	I_{max} (%)	EC_{50}(μM)	n_H	I_{max} (%)
GABA	1.19 ± 0.02	2.2 ± 0.1	99.7 ± 0.5	1.03 ± 0.05	2.0 ± 0.2	98.4 ± 1.3	3.6 ± 0.2	1.6 ± 0.1	98.4 ± 1.6
(+)-CAMP	39.7 ± 1.3[a]	2.1 ± 0.2[a]	104.0 ± 1.0[a]	16.6 ± 2.1[a]	1.5 ± 0.3[a]	108.0 ± 1.0[a]	28.1 ± 0.3	2.4 ± 0.1	69.4 ± 0.3
(−)-CAMP	IC_{50} = 890 ± 150 μM[a]			IC_{50} = 400 ± 80 μM[a]			IC_{50} = 178 ± 48 μM		
(*S*)-2-MeGABA	64.6 ± 2.9	2.3 ± 0.2	97.5 ± 1.7	19.8 ± 1.3	1.4 ± 0.1	102.1 ± 1.9	24.7 ± 1.0	2.0 ± 0.1	89.6 ± 1.3
(*R*)-2-MeGABA	IC_{50} = 15.9 ± 1.6 μM		IC_{50} = 125.0 ± 11.2 μM	IC_{50} = 35.8 ± 5.4 μM					
(+)-ACPECA	134.7 ± 8.2	1.8 ± 0.2	98.6 ± 2.7	61.0 ± 2.8	2.5 ± 0.2	97.8 ± 1.6	112.3 ± 2.2	2.5 ± 0.2	37.3 ± 0.4
(−)-ACPECA	300 μM inhibits 23.1 ± 4.9% of the current produced by 1 μM GABA (Fig. 4)			ND[b]		300 μM inhibits 15.1 ± 6.1% of the current produced by 3 μM GABA (Fig. 4)			

[a] Data from Duke et al.[1]

[b] Percentage inhibition value was not determined as the whole cell current was too low.

a moderate, full agonist at ρ1 and ρ2 receptors (EC_{50} = 134.7 μM, I_{max} = 98.6% and EC_{50} = 61.0 μM, I_{max} = 97.8%, respectively) and a moderate, partial agonist at ρ3 (EC_{50} = 112.3 μM; I_{max} = 37.3%). (−)-ACPECA was a weak antagonist at all three receptor subtypes, with an IC_{50} above 300 μM. 300 μM (−)-ACPECA produced 23% inhibition of the 1 μM GABA current at the ρ1 receptor (Fig. 4a) and 15% of the 3 μM GABA current at the ρ3 receptor (Fig. 4b). Due to the low whole-cell currents produced by the ρ2 receptors, the degree of inhibition produced by application of 300 μM was not numerically significant and hence is not reported here.

3. Discussion

Conformationally restricted GABA analogues have long been used to probe structure–activity relationships at $GABA_C$ receptors.[15,16,18–20] However, the majority of these studies have used racemic mixtures of chiral compounds rather than testing the enantiomerically resolved isomers. Here, we examine *cis*-constrained and flexible 2-substituted GABA analogues that can attain a *cis* conformation. Previous studies at ρ1 $GABA_C$ receptors have shown that a racemic mixture of 2-MeGABA possesses both weak partial agonist ($EC_{50} \approx 189$ μM, $I_{max} \approx 12\%$) and moderate antagonist ($IC_{50} \approx 53$ μM) activity.[16] A racemic mixture of CAMP was found to exhibit potent full agonist activity ($EC_{50} \approx 65$ μM, $I_{max} \approx 110\%$). In these cases, the observed biological response corresponds to the combined effects of both enantiomers and the contribution of each individual enantiomer to the overall biological response is unclear. Subsequent studies,[1] however, established that enantiomers of the *cis*-constrained chiral GABA analogue (±)-CAMP have different biological activities to the racemic mixture, with the enantiomers exhibiting opposite pharmacological activity at recombinant ρ1 and ρ2 GABA receptors. This is an interesting result, because although enantiomers of chiral compounds are well known for exerting different physiological effects in a number of biological systems,[21,22] it is rare that opposite effects are observed at a single target site.[1,23,24]

Having established that the enantiomers of (±)-CAMP exhibit opposite effects at $GABA_C$ receptors, it is interesting to consider whether other *cis*-constrained and flexible 2-substituted GABA analogues that can attain a *cis* conformation will exhibit similar behaviour. The results presented in this study, therefore, represent an extension of the previous investigation to include the effects of a larger range of *cis*-constrained and flexible 2-substituted chiral GABA analogues. Furthermore, the results are reported for the human ρ1 and ρ2 subtypes of the recombinant $GABA_C$ receptor, in addition to the rat ρ3 subtype.

In analogy to the opposite pharmacological effects of (+)-CAMP and (−)-CAMP, (+)- ACPECA was found to act as an agonist at all three subtypes of $GABA_C$ receptor, while its enantiomeric pair (−)-ACPECA was a weak antagonist. Similarly, (*S*)-2MeGABA activated

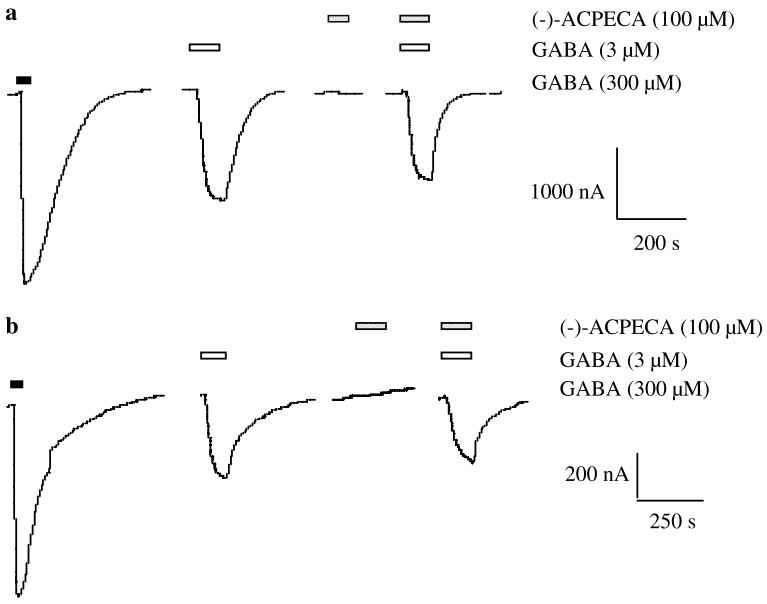

Figure 4. (a) A maximal current is achieved by application of GABA (100 μM; duration indicated by the solid bar) on *Xenopus* oocytes expressing ρ1 $GABA_C$ receptors. A submaximal current is achieved by the addition of GABA (1 μM, duration indicated by open bar). (−)-ACPECA had no effect when administered alone (300 μM, duration indicated by hatched bar), but decreased the response to GABA (1 μM, duration indicated by open bar) by 23% when co-administered (300 μM, duration indicated by hatched bar). (b) A maximal current is achieved by application of GABA (300 μM; duration indicated by the solid bar) on *Xenopus* oocytes expressing ρ3 $GABA_C$ receptors. A submaximal current is achieved by the addition of GABA (3 μM, duration indicated by open bar). (−)-ACPECA had no effect when administered alone (300 μM, duration indicated by hatched bar), but decreased the response to GABA (3 μM, duration indicated by open bar) by 15% when co-administered (300 μM, duration indicated by hatched bar).

$GABA_C$ receptors, whereas (*R*)-2MeGABA had moderately potent blocking effects.

These results raise the question of why enantiomers of chiral GABA analogues exert opposite effects at $GABA_C$ receptors. To answer this question, it is necessary to determine the in vivo structures of these compounds as a basis for subsequent structure-activity relationship studies. As the mammalian body is a predominantly aqueous environment, it is reasonable to assume that the in vivo structure can be closely approximated by the aqueous solution-phase structure. In the absence of any direct experimental data about the three-dimensional structure of the $GABA_C$ receptor binding site, which would allow us to account for environmental influence on the ligand conformation, we also assume that the binding conformation can be approximated by the aqueous phase structure. The lowest energy conformers, obtained by geometry optimization at MP2/6-31+G* within the COSMO continuum solvation model, are illustrated in Figure 5. From this figure, we observe that all three compounds exist as folded, intramolecularly hydrogen-bonded conformers in aqueous solution.

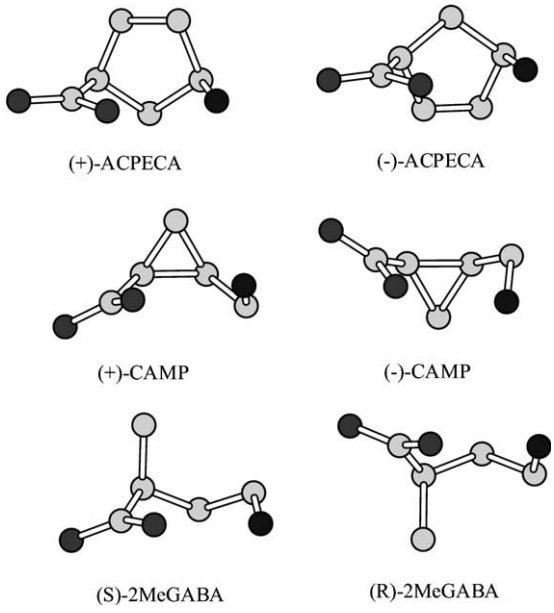

Figure 5. MP2/6-31+G* optimized, solution-phase structures of (+)-CAMP, (−)-CAMP, (+)-ACPECA, (−)-ACPECA, (*S*)-2MeGABA and (*R*)-2MeGABA. The atoms are depicted as greyscale circles. Oxygen atoms are dark grey, carbon atoms are light grey and nitrogen atoms are black. For clarity, hydrogen atoms are not illustrated here.

Superposition of the carboxylate group and amine group of the cyclopropane analogues with the equivalent residues on the cyclopentene analogues reveals that both enantiomers of the cyclopropane analogues are superposable on each of the cyclopentene analogues, as shown in Figure 6. The cyclopentene analogues were chosen as template molecules as they are the most conformationally restricted of all the GABA analogues studied here and therefore define a unique pharmacophoric pattern. Conceptually, this implies that both (+)-CAMP and (−)-CAMP fit an agonist binding profile, since each enantiomer is superposable on the more conformationally restricted agonist (+)-ACPECA. However, both enantiomers also fit an antagonist

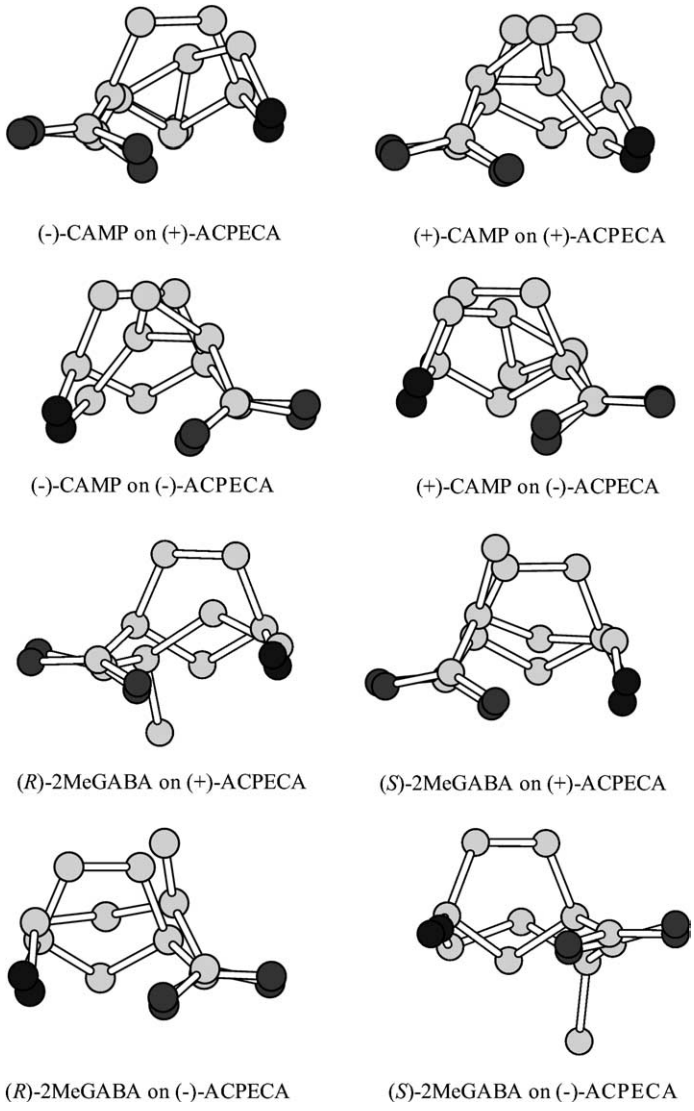

Figure 6. Superpositions of (+)-CAMP (agonist), (−)-CAMP (antagonist), (*S*)-2MeGABA (agonist) and (*R*)-2MeGABA (antagonist) onto (+)-ACPECA (agonist) and (−)- ACPECA (antagonist). The atoms are depicted as greyscale circles as in Figure 5.

binding profile, since each enantiomer is also superposable on (−)-ACPECA. Therefore, the opposite biological activities of the enantiomers of CAMP, 2-Me-GABA and ACPECA must arise from stereoselective steric interactions at the $GABA_C$ receptor binding site. We illustrate this concept by considering the binding of (+)-CAMP and (−)-CAMP to a putative receptor model.

First, it is reasonable to assume that both the amino and carboxylate termini bind to amino acid residues at the binding site. The positively charged amino group will bind to negatively charged, negatively polarized and aromatic amino acids, whereas the negatively charged carboxylate group will bind to positively charged or polarized amino acids. For reference, we choose to depict the binding sites in the plane of the page with the carboxylate binding site on the left and the amino binding site on the right, although this frame of reference is arbitrary. Both orientations (+)-CAMP and (−)-CAMP could attain at the binding site are shown in Figures 7a and b, respectively.

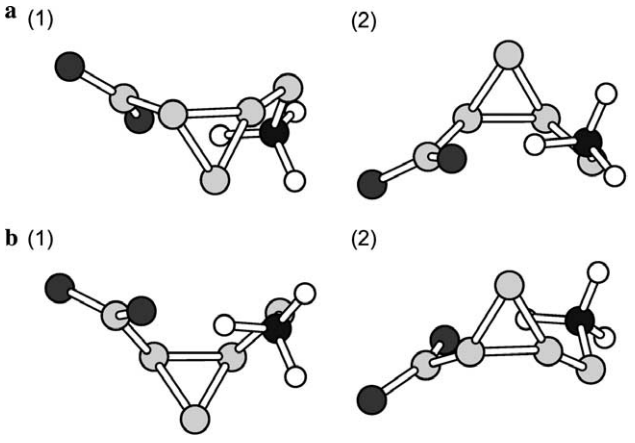

Figure 7. (a) Both possible orientations (+)-CAMP could attain at the binding site. Orientation 2 is preferred over orientation 1 on the basis of minimizing steric interactions. (b) Both possible orientations (−)-CAMP could attain at the binding site. Orientation 2 is preferred over orientation 1 on the basis of minimizing steric interactions.

Without introducing any constraints to determine ligand orientation, (+)-CAMP conformer 2 and (−)-CAMP conformer 1 both fit an agonist binding profile (as defined by the binding of (+)-ACPECA), whereas (+)-CAMP conformer 1 and (−)-CAMP conformer 2 fit an antagonist binding profile. Therefore, we introduce the notion of an excluded volume around the binding site, which acts to orientate the steric bulk of each conformer 'up' and away from the binding site. Again, this choice of directionality is arbitrary; a constraint which results in the alternative orientation would be equally valid. This results in the exclusion of (+)-CAMP conformer 1 and (−)-CAMP conformer 1 as potential binding conformers, leaving (+)-CAMP conformer 2 and (−)-CAMP conformer 2 bound to the model receptor binding site as shown in Figure 8. From this figure, we observe that (+)-CAMP binds such that the bulk of the molecule is behind the plane of the page, and we postulate that this spatial arrangement leads to agonist activity. In contrast, (−)-CAMP binds such that the bulk of the molecule is in front of the plane of the page, and we postulate that this spatial arrangement leads to antagonist activity.

This rationale is also consistent with the data obtained for the cyclopentene analogues and the 2-methyl substituted analogues. According to this model, (+)-ACPECA and (*S*)-2-MeGABA are orientated at the binding site such that the bulk of the molecule is behind the plane of the page, and (−)-ACPECA and (*R*)-2MeGABA are orientated such that the bulk of the molecule is in front of the plane of the page. Hence, (+)-ACPECA and (*S*)-2MeGABA are agonists, while (−)-ACPECA and (*R*)-2MeGABA are antagonists.

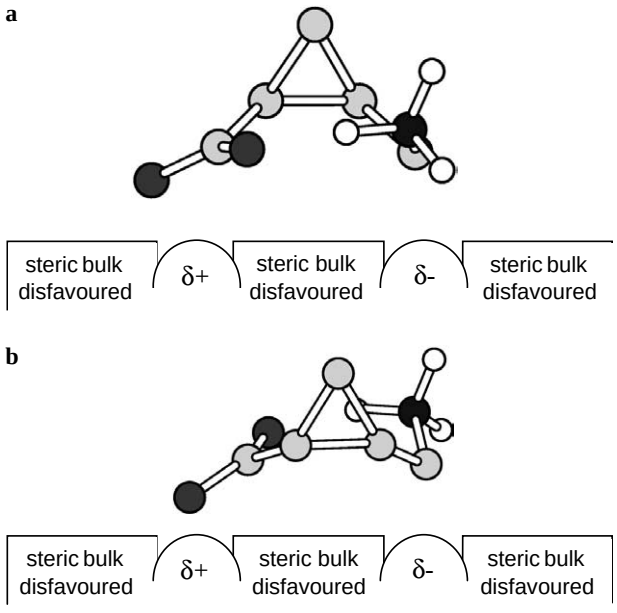

Figure 8. (a) Preferred agonist binding conformation, illustrated by (+)-CAMP. The amino and carboxylate termini are in the plane of the page and the bulk of the molecule is behind the plane of the page. This spatial arrangement results in subsequent agonist activity. (b) Preferred antagonist binding conformation, illustrated by (−)-CAMP. The amino and carboxylate termini are in the plane of the page and the bulk of the molecule is in front of the plane of the page. This spatial arrangement results in subsequent antagonist activity.

Although (+)-CAMP, (+)-ACPECA and (*S*)-2MeGABA have agonist activity at all three receptor subtypes, they act as full agonists at the ρ1 and ρ2 receptors but with varying degrees of partial agonist activity at ρ3 receptors. (*S*)-2MeGABA, the most conformationally flexible analogue considered here, is almost a full agonist at ρ3, with a maximal intrinsic activity of 90%. Increasing the conformational rigidity to obtain (+)-CAMP resulted in a corresponding decrease in agonist activity to a maximal response of approximately 70%. Further increasing the conformational rigidity, in the case of (+)-ACPECA, resulted in a further decrease in agonist activity to a maximal response of 50%. These results suggest that conformational flexibility may be particularly important at the binding site of ρ3 receptors in determining the maximal response. However, the series GABA, 2-Me-GABA, (+)-CAMP and (+)-ACPECA also exhibits increasing steric bulk and this may also affect the degree of motion that the molecule can undergo at the binding site, and hence influence the maximal response. Further elucidating these factors: conformational flexibility and steric bulk, will provide important clues to the nature of the $GABA_C$ ρ3 receptor binding site.

In conclusion, we have examined the structure–activity relationships of a number of optically pure, chiral GABA analogues and proposed a novel mechanism for the genesis of the stereoselectivity effect, on the basis of solution-phase structures obtained at the MP2/6-31+G* level of ab initio theory. This model predicts that the binding orientation is determined by competing steric interactions, either upon approach to or at the binding site, and that this is the major influence contributing to the orientation of the molecule at the binding site.

4. Materials and methods

4.1. Materials

The compounds depicted in Figure 1 were synthesized according to literature methods.[25–27] GABA was purchased from Sigma (St. Louis, MO, USA). Human ρ1 cDNA subcloned in pcDNA1.1 (Invitrogen, San Diego, CA, USA) was kindly provided by Dr. George Uhl (National Institute for Drug Abuse, Baltimore, MD, USA). Human ρ2 subcloned in pKS (invitrogen) was kindly donated by Dr. Garry Cutting (Center for Medical Genetics, Johns Hopkins University School of Medicine, Baltimore, MD, USA). Rat ρ3 cDNA subcloned in pBluescript KS (−) (invitrogen) was kindly donated by Professor Ryozu Shingai (Department of Information Science, Faculty of Engineering, Iwate University, Japan).

4.2. Methods

4.2.1. Experimental. *Xenopus laevis* were anaesthetized with 0.17% ethyl-3-aminobenzoate, and a lobe of the ovaries was removed. The lobe of the ovary was rinsed

with oocyte-releasing buffer 2 (OR2) (82.5 mM NaCl, 2 mM KCl, 1 mM $MgCl_2{\cdot}6H_2O$ and 5 mM HEPES, pH 7.5) and treated with collagenase A (2 mg/mL in OR2, Boehringer Mannheim) for 2 h. Released oocytes were then rinsed in frog Ringer buffer (96 mM NaCl, 2 mM KCl, 1 mM $MgCl_2{\cdot}6H_2O$, 1.8 mM $CaCl_2$ and 5 mM HEPES, pH 7.5) supplemented with 2.5 mM pyruvate, 0.5 mM theophylline and 50 mg/mL gentamycin and stage V–VI oocytes were collected.

Separate batches of human ρ1 and ρ2 and rat ρ3 cRNA were prepared according to literature methods.[15,20] Human ρ1 cDNA subcloned in pcDNA1.1 was linearized with the *Xba*I restriction enzyme and cRNA was synthesized using the 'T7 polymerase mMESSAGE mMACHINE' kit (Ambion, Austin, TX, USA). Human ρ2 cDNA subcloned in pcKS was linearized with the *Eco*RV restriction enzyme and cRNA was synthesized using the 'T7 polymerase mMESSAGE mMACHINE' kit (Ambion, Austin, TX, USA). Rat ρ3 cDNA subcloned in pBluescript KS(−) was linearized with the *Eco*R1 restriction enzyme and cRNA was synthesized using the 'T3 polymerase mMESSAGE mMACHINE' kit from (Ambion, Austin, TX, USA).

10 ng in 50 nL of ρ1 cRNA, 50 ng/50nL of ρ2 cRNA and 50 ng/50 nL of ρ3 cRNA were injected into the defolliculated stage V–VI *Xenopus* oocytes. Oocytes were incubated at 15 °C for 2–4 days and then allowed to warm to room temperature before receptor activity was measured by two-electrode voltage-clamp recording using a GeneClamp 500 Amplifier (Axon Instruments, Foster City, CA, USA), a MacLab 2e recorder (AD instruments, Sydney, NSW, Australia) and Chart program, version 3.6.3. Oocytes were voltage-clamped at −60 mV and continously superfused with frog Ringer buffer. For receptor activation measurements, the indicated concentrations of drug were added to the buffer solution. The flow rate of the solution was set to 5 mL/min and the drug doses were applied at 30 min intervals.

4.3. Computational

Geometry optimizations were carried out on the compounds shown in Figure 1 using the second-order Moller–Plesset Perturbation Theory (MP2),[28–31] utilizing a 6-31+G* basis set.[32–36] Short-range solvent interactions were accounted for by including two explicit water molecules in the geometry optimization process. Long range solvent interactions were modelled by reoptimization within the COSMO dielectric continuum model.[37,38] Conformational space was explored by rotation in 10° increments about non-constrained bonds in (*R*)-2MeGABA, (*S*)-2MeGABA, (+)-CAMP and (−)-CAMP. Where local minima were identified on the torsional potentials, these geometries were then isolated and reoptimized within the COSMO dielectric continuum model. This approach has previously been validated for the determination of solution-phase structures of biological zwitterions, where the solvated structures were found to be similar irrespective of whether an explicit hydration model or bulk solvation model was used to incorporate solvent effects.[39] The resultant low-energy structures were compared by superimposing the amine and carboxylic acid groups of each compound.

All calculations were carried out using the GAUSSIAN03 program suite[40] on the computing facilities at the Australian Partnership for Advanced Computing (APAC) National Facility, based at the Australian National University.

4.4. Data analysis

Electrophysiological recordings generated data in the form of current (*I*) versus agonist concentration [A]. These data were standardized by calculating the responses as percentages of the maximum, according to the equation: $\%I = I/I_{max} \times 100$. These data were then fit by least squares to the Hill equation:

$$\%I = \frac{I_{max}[A]^{n_H}}{EC_{50}^{n_H} + [A]^{n_H}},$$

where I_{max} is the maximal percentage response, EC_{50} is the agonist concentration which elicits 50% of the maximum response, and n_H is the Hill coefficient. The intrinsic activity of partial agonists, I_{max}, was calculated as a percentage of the maximum current produced by a maximum dose of GABA.

Acknowledgments

We are grateful to Dr. George Uhl (Baltimore, MD, USA), Dr Gary Cutting (Baltimore, MD, USA) and Professor Ryozu Shingai (Iwate, Japan) for gifts of ρ1, ρ2 and ρ3 cDNA, respectively. We would also like to thank Drs. Hue Tran, Erica Campbell, Mr. Kong Li and Ms. Suzanne Habjan for harvesting the oocytes used in receptor activation measurements and Ms. Jane Carland for preparing the human ρ1 and ρ2 mRNA. Financial support for this work, provided by the Australian National Health and Medical Research Council and the U.S. National Institute of Health (GM66132 to R.B.S.), is gratefully acknowledged. This work has also been supported by a grant of supercomputer time by the Australian Partnership for Advanced Computing Merit Allocation Scheme.

References and notes

1. Duke, R. K.; Chebib, M.; Balcar, V. J.; Allan, R. D.; Mewett, K. N.; Johnston, G. A. R. *J. Neurochem.* **2000**, *75*, 2602–2610.
2. Murata, Y.; Woodward, R. M.; Miledi, R.; Overman, L. E. *Bioorg. Med. Chem. Lett.* **1996**, *6*, 964–968.
3. Ragozzino, D.; Woodward, R. M.; Murata, Y.; Eusebi, F.; Overman, L. E.; Miledi, R. *Mol. Pharmacol.* **1996**, *50*, 1024–1030.
4. Amin, J.; Weiss, D. *Receptors Channels* **1994**, *2*, 227–236.
5. Kusama, T.; Spivak, C. E.; Whiting, P.; Dawson, V. L.; Schaeffer, J. C.; Uhl, G. R. *Br. J. Pharmacol.* **1993**, *109*, 200–206.
6. Cutting, G. R.; Curristin, S.; Zoghbi, H.; O'Hara, B.; Seldin, M. F.; Uhl, G. R. *Genomics* **1992**, *12*, 801–806.

7. Cutting, G. R.; Lu, L.; O'Hara, B. F., et al. *Proc. Natl. Acad. Sci. U.S.A.* **1991**, *88*, 2673–2677.
8. Ogurusu, T.; Shingai, R. *Biochim. Biophys. Acta* **1996**, *1305*, 15–18.
9. Ogurusu, T.; Taira, H.; Shingai, R. *J. Neurochem.* **1995**, *65*, 964–968.
10. Wang, T.-L.; Guggino, W. B.; Cutting, G. R. *J. Neurosci.* **1994**, *14*, 6524–6531.
11. Zhang, D.; Pan, Z. H.; Zhang, X.; Brideau, A.; Lipton, S. A. *Proc. Natl. Acad. Sci. U.S.A.* **1995**, *92*, 11756–11760.
12. Enz, R.; Brandstatter, J. H.; Hartveit, E.; Wassle, H.; Bormann, J. *Eur. J. Neurosci.* **1995**, *7*, 1495–1501.
13. Boue-Grabot, E.; Roudbaraki, M.; Bascles, L.; Tramu, G.; Bloch, B.; Garret, M. *J. Neurochem.* **1998**, *70*, 899–907.
14. Wegelius, K.; Pasternack, M.; Hiltunen, J. O.; Rivera, C.; Kaila, K.; Saarma, M.; Reeben, M. *Eur. J. Neurosci.* **1998**, *10*, 350–357.
15. Vien, J.; Duke, R. K.; Mewett, K. N.; Johnston, G. A. R.; Shingai, R.; Chebib, M. *Br. J. Pharmacol.* **2001**, *135*, 883–890.
16. Chebib, M.; Vandenberg, R. J.; Johnston, G. A. R. *Br. J. Pharmacol.* **1997**, *122*, 1551–1560.
17. Kusama, T.; Wang, T.-L.; Guggino, W. B.; Cutting, G. R.; Uhl, G. R. *Eur. J. Pharmacol.* **1993**, *245*, 83–84.
18. Chebib, M.; Vandenberg, R. J.; Froestl, W.; Johnston, G. A. R. *Eur. J. Pharmacol.* **1997**, *329*, 223–229.
19. Chebib, M.; Duke, R. K.; Allan, R. D.; Johnston, G. A. R. *Eur. J. Pharmacol.* **2001**, *430*, 185–192.
20. Stinson, S. C. *Chem. Eng. News* **1998**, *21*, 83–104.
21. Thall, E. *J. Chem. Ed.* **1996**, *73*, 481–484.
22. Ebert, B.; Lenz, S.; Brehm, L.; Bregnadel, P.; Hansen, J. J.; Frederiksen, K.; Bogeso, K. P.; Krogsgaard-Larsen, P. *J. Med. Chem.* **1994**, *37*, 878–884.
23. Hacksell, U. In *A Textbook of Drug Design and Development*; Krogsgaard-Larsen, P., Bundgaard, H., Eds.; Harwood Academic: Chur, 1996, pp 48–52.
24. Duke, R. K.; Allan, R. D.; Chebib, M.; Greenwood, J. R.; Johnston, G. A. R. *Tetrahedron: Asymmetry* **1998**, *9*, 2533–2548.
25. Duke, R. K.; Chebib, M.; Hibbs, D. E.; Mewett, K. N.; Johnston, G. A. R. *Tetrahedron: Asymmetry* **2004**, *15*, 1745–1751.
26. Qiu, J.; Silverman, R. B. *J. Med. Chem.* **2000**, *43*, 706–720.
27. Chebib, M.; Mewett, K. N.; Johnston, G. A. R. *Eur. J. Pharmacol.* **1998**, *357*, 227–234.
28. Bartlett, R. J.; Purvis, G. D. *Int. J. Quantum Chem.* **1978**, *14*, 561–581.
29. Bartlett, R. J.; Silver, D. M. *J. Chem. Phys.* **1975**, *62*, 3258–3268.
30. Krishnan, R.; Pople, J. A. *Int. J. Quantum Chem.* **1978**, *14*, 91–100.
31. Pople, J. A.; Binkley, J. S.; Seeger, R. *Int. J. Quantum Chem. Quantum Chem. Symp.* **1976**, *10*, 1–10.
32. Clark, T.; Chandrasekhar, J.; Spitznagel, G. W.; Schleyer, P. v. R. *J. Comput. Chem.* **1983**, *4*, 294–301.
33. Ditchfield, R.; Hehre, W. J.; Pople, J. A. *J. Chem. Phys.* **1971**, *54*, 724–728.
34. Hariharan, P. C.; Pople, J. A. *Theor. Chem. Acta* **1973**, *28*, 213–222.
35. Hehre, W. J.; Ditchfield, R.; Pople, J. A. *J. Chem. Phys.* **1972**, *56*, 2257–2261.
36. Spitznagel, G. W.; Clark, T.; Chandrasekhar, J.; Schleyer, P. v. R. *J. Comput. Chem.* **1982**, *3*, 363–371.
37. Klamt, A. In *Encyclopedia of Computational Chemistry;* J. Wiley & Sons: Chichester, 1998; pp 604–615.
38. Klamt, A.; Schuurmann, G. *J. Chem. Soc., Perkin Trans. 2* **1993**, 799–805.
39. Crittenden, D. L.; Chebib, M.; Jordan, M. J. T. *J. Phys. Chem. A* **2004**, *108*, 203–211.
40. Frisch, M. J.; Trucks, G. W.; Schlegel, H. B.; Scuseria, G. E.; Robb, M. A.; Cheeseman, J. R.; Montgomery, J. A., Jr.; Vreven, T.; Kudin, K. N.; Burant, J. C.; Millam, J. M.; Iyengar, S. S.; Tomasi, J.; Barone, V.; Mennucci, B.; Cossi, M.; Scalmani, G.; Rega, N.; Petersson, G. A.; Nakatsuji, H.; Hada, M.; Ehara, M.; Toyota, K.; Fukuda, R.; Hasegawa, J.; Ishida, M.; Nakajima, T.; Honda, Y.; Kitao, O.; Nakai, H.; Klene, M.; Li, X.; Knox, J. E.; Hratchian, H. P.; Cross, J. B.; Bakken, V.; Adamo, C.; Jaramillo, J.; Gomperts, R.; Stratmann, R. E.; Yazyev, O.; Austin, A. J.; Cammi, R.; Pomelli, C.; Ochterski, J. W.; Ayala, P. Y.; Morokuma, K.; Voth, G. A.; Salvador, P.; Dannenberg, J. J.; Zakrzewski, V. G.; Dapprich, S.; Daniels, A. D.; Strain, M. C.; Farkas, O.; Malick, D. K.; Rabuck, A. D.; Raghavachari, K.; Foresman, J. B.; Ortiz, J. V.; Cui, Q.; Baboul, A. G.; Clifford, S.; Cioslowski, J.; Stefanov, B. B.; Liu, G.; Liashenko, A.; Piskorz, P.; Komaromi, I.; Martin, R. L.; Fox, D. J.; Keith, T.; Al-Laham, M. A.; Peng, C. Y.; Nanayakkara, A.; Challacombe, M.; Gill, P. M. W.; Johnson, B.; Chen, W.; Wong, M. W.; Gonzalez, C.; Pople, J. A. Gaussian 03, Revision C.02, Gaussian, Wallingford CT, 2004.